MCB
Journals.ASM.org

The Preference for Error-Free or Error-Prone Postreplication Repair in *Saccharomyces cerevisiae* Exposed to Low-Dose Methyl Methanesulfonate Is Cell Cycle Dependent

Dongqing Huang,[a] Brian D. Piening,[b] Amanda G. Paulovich[a]

Fred Hutchinson Cancer Research Center, Seattle, Washington, USA[a]; Molecular and Cellular Biology Program, University of Washington, Seattle, Washington, USA[b]

Cells employ error-free or error-prone postreplication repair (PRR) processes to tolerate DNA damage. Here, we present a genome-wide screen for sensitivity to 0.001% methyl methanesulfonate (MMS). This relatively low dose is of particular interest because wild-type cells exhibit no discernible phenotypes in response to treatment, yet PRR mutants are unique among repair mutants in their exquisite sensitivity to 0.001% MMS; thus, low-dose MMS treatment provides a distinctive opportunity to study postreplication repair processes. We show that upon exposure to low-dose MMS, a PRR-defective *rad18*Δ mutant stalls into a lengthy G_2 arrest associated with the accumulation of single-stranded DNA (ssDNA) gaps. Consistent with previous results following UV-induced damage, reactivation of Rad18, even after prolonged G_2 arrest, restores viability and genome integrity. We further show that PRR pathway preference in 0.001% MMS depends on timing and context; cells preferentially employ the error-free pathway in S phase and do not require *MEC1*-dependent checkpoint activation for survival. However, when PRR is restricted to the G_2 phase, cells utilize *REV3*-dependent translesion synthesis, which requires a *MEC1*-dependent delay and results in significant hypermutability.

The DNA damage response (DDR) employs a signal transduction network to delay cell cycle progression and promote DNA repair (1). While it is well known that DNA damage checkpoints are critical for maintaining genome integrity, how the cell balances between checkpoint arrest and cell proliferation in the setting of constant endogenous and exogenous sources of DNA damage (~20,000 lesions per day per human cell) remains a critical question (2, 3). For example, cells utilize excision repair and DNA damage tolerance pathways without significant delay of the cell cycle to address low levels of DNA damage (such as spontaneous base lesions), yet when responding to a higher level of DNA damage, these processes become tightly integrated with cell cycle delay (1). For genotoxic agents, there is a dose threshold below which checkpoint activation is minimal despite measurable activity of DNA repair pathways (4, 5); this threshold may vary, depending on the damaging agent, organism, and cell type. We (6) and others (4) have described novel cellular phenotypes that manifest only in response to low doses of DNA-damaging agents; however, the field lacks a consistent definition of what constitutes a low dose. To generalize this phenomenon, we propose the definition of a "low dose" of a damaging agent as a treatment condition that does not cause discernible DNA damage sensitivity in treated wild-type cells yet manifests discernible biological effects (such as sensitivity) in mutant genetic backgrounds. While other definitions are equally valid, this definition is not agent specific and thus allows for a comparison of results spanning multiple genotoxic agents. Our use of the terms "low dose" and "high dose" in this study refers to this distinction.

DNA-alkylating agents (methyl methanesulfonate [MMS], ethylmethanesulfonate [EMS], melphalan, etc.) are of particular interest at low doses, as this class of genotoxic agents encompasses a number of natural and industrial environmental carcinogens (2). Alkylating agents induce DNA damage by transferring methyl groups to oxygen or nitrogen atoms of DNA bases, resulting in highly mutagenic DNA base lesions, such as O^6-methylguanine and N^3-methyladenine (2, 7). Use of such agents at high doses (most prominently the monofunctional agent MMS) have aided in the discovery of novel DDR genes and the elucidation of many biochemical processes underlying the DDR (8–11). While these studies have relied specifically on high doses of MMS, there is reason to believe that the cellular response to exposure to a low dose of MMS is executed differently (5, 6).

Recent work has begun to characterize the differences between low- and high-dose DNA damage responses (4, 6). In a recent study chronicling novel, low-dose-specific DDR phenotypes, Hishida et al. continuously exposed yeast cells to low-dose UV light (0.1 J/m^2/min) over a period of multiple days in order to mimic how yeast might cope with sunlight-induced UV damage in the wild (4). They tested a panel of strains defective for different components of DDR pathways, and the results were striking: only mutants comprising members of postreplicative repair (PRR) pathways exhibited any sensitivity to chronic low-dose UV treatment, and despite this, the sensitivity of these mutants was extreme. Moreover, they showed that while wild-type cells cycle normally in low-dose UV, a PRR-defective *rad18*Δ mutant rapidly synchronizes into prolonged G_2 arrest (4).

PRR facilitates the bypass (rather than the repair) of base lesions through either an error-prone polymerase switch or an error-free template switch mechanism (12–14). The polymerase switch pathway involves a switch to an error-prone translesion synthesis (TLS) polymerase that can catalyze DNA synthesis

Received 15 October 2012 Returned for modification 15 November 2012
Accepted 30 January 2013
Published ahead of print 4 February 2013
Address correspondence to Amanda G. Paulovich, apaulovi@fhcrc.org.

doi:10.1128/MCB.01392-12

across a damaged template by inserting a noncognate nucleotide (13–15). In contrast, the template switch mechanism is error free and utilizes the newly synthesized sister chromatid as a template for DNA synthesis across the damaged base (13, 14, 16). Both pathways are initiated by the Rad6/Rad18-mediated ubiquitination of PCNA; the monoubiquitination of PCNA at K164 triggers TLS; however if this site is further polyubiquitinated by Ubc13-Mms2-Rad5, the cell instead employs an error-free template switch (12). The conditions that determine PRR pathway choice are not yet understood.

While the work of Hishida et al. has chronicled the requirement for PRR for survival under chronic low-dose UV treatment conditions, significant questions remain. It is unknown whether this PRR reliance is low-dose UV specific or if it extends to low doses of other DNA-damaging agents. Moreover, Hishida et al. screened a small panel of known DNA repair mutants for low-dose UV sensitivity; it is unknown whether genes outside this panel of canonical DNA repair genes are also required for survival under low-dose conditions. If under low-dose conditions the PRR pathway is predominantly responsible for cell survival, then this genotoxic context presents a tremendous opportunity for detailed studies of PRR mechanisms with minimal competition from repair processes and without the need for additional mutations.

In order to address these outstanding questions, we performed the first genome-wide screen for mutants that cause sensitivity to low-dose MMS. We show that mutants in PRR pathways are exquisitely sensitive to 0.001% MMS, while mutants that function in end resection and homologous recombination (HR)-intermediate processing exhibit only mild sensitivity. We show that in low-dose MMS, loss of PRR function is associated with prolonged G_2 arrest that is likely due to unrepaired single-stranded DNA (ssDNA) gaps occurring during DNA replication. Reactivation of PRR during this arrest restores cell viability, restarts cell cycle progression, and restores ssDNA to intact chromosomal double-stranded DNA (dsDNA) but results in significant mutagenesis. We show that, unlike PRR during the S phase, which favors the error-free pathway, delayed PRR activation results in DNA repair predominantly by error-prone translesion synthesis. Elucidation of these phenotypes was made possible by specifically utilizing continuous low-dose MMS treatment, in which S-phase progression is unaffected and wild-type cells rely on tolerance pathways to facilitate DNA replication.

MATERIALS AND METHODS

Strains, medium, and growth conditions. The *S. cerevisiae* strains used in this study are listed in Table 1. Strain BY4741 was obtained from Open Biosystems. All of the other strains used in this study are derived from BY4741. YPD medium contains 1% yeast extract, 2% peptone, and 2% glucose. YPG medium contains a 2% concentration of galactose to induce the expression of genes under the control of the *pGAL1* promoter. MMS was purchased from Acros Organics (AC254609). YPD plates containing MMS were prepared approximately 15 h prior to use.

Gene disruptions and integrations. All gene disruptions and integrations were achieved by homologous recombination at their respective chromosomal loci by standard PCR-based methods (17). Briefly, a deletion cassette with a 0.5-kb region flanking the target open reading frame (ORF) was amplified by PCR from the corresponding *xxx*Δ::*KANMX* strain of the deletion array (Open Biosystems) and transformed into the target strain for gene knockout. The primers used in the gene disruptions were designed using 20-bp sequences that are 0.5 kb upstream and downstream of the target gene (18).

TABLE 1 *Saccharomyces cerevisiae* strains

Strain[a]	Genotype	Source
BY4741	*MATa his3Δ1 leu2Δ0 met15Δ0 ura3Δ0*	Open Biosystems
yDH125	*MATa BY4741 mec1*ΔKAN^r *sml1*ΔNAT^r	This study
yDH143	*MATa BY4741 rev3*ΔNAT^r	This study
yDH156	*MATa BY4741 rad9*ΔKAN^r *rad57*ΔNAT^r	This study
yDH157	*MATa BY4741 mag1*ΔKAN^r *rad57*ΔNAT^r	This study
yDH159	*MATa BY4741 mag1*ΔKAN^r *rad9*ΔNAT^r	This study
yDH162	*MATa BY4741 pGAL-RAD18::HIS3MX6*	This study
yDH179	*MATa BY4741 pGAL-RAD18::HIS3MX6 rad57*ΔKAN^r	This study
yDH183	*MATa BY4741 sml1*ΔNAT^r *mec1ΔHIS3MX6 mms2*ΔKAN^r	This study
yDH184	*MATa BY4741 sml1*ΔNAT^r *mec1ΔHIS3MX6 rev3*ΔKAN^r	This study
yDH215	*MATa BY4741 rad18*ΔKAN^r *pGAL-RAD57::HIS3MX6*	This study
yDH227	*MATa BY4741 rad18*ΔKAN^r	This study
yDH231	*MATa BY4741 rad18*ΔKAN^r *rad57*ΔNAT^r	This study
yDH237	*MATa BY4741 rad9*ΔNAT^r *rad18*ΔKAN^r	This study
yDH240	*MATa BY4741 rad18*ΔNAT^r *mag1*ΔKAN^r	This study
yDH253	*MATa BY4741 pGAL-RAD18::HIS3MX6 mms2*ΔKAN^r	This study
yDH254	*MATa BY4741 pGAL-RAD18::HIS3MX6 rev3*ΔKAN^r	This study
yDH341	*MATa BY4741 srs2*ΔNAT^r *rad18*ΔKAN^r *pGAL-RAD57::HIS3MX6*	This study
yDH342	*MATa BY4741 mms2*ΔKAN^r *rev3*ΔNAT^r	This study
yDH343	*MATa BY4741 mec1*ΔKAN^r *sml1*ΔNAT^r *pGAL-RAD18::HIS3MX6*	This study
yDH346	*MATa BY4741 rad6*ΔKAN^r	This study
yDH347	*MATa BY4741 rad57*ΔKAN^r	This study
yDH348	*MATa BY4741 rad52*ΔKAN^r	This study
yDH349	*MATa BY4741 mag1*ΔKAN^r	This study
yDH350	*MATa BY4741 rad9*ΔKAN^r	This study
yDH352	*MATa BY4741 top3*ΔKAN^r	This study
yDH353	*MATa BY4741 rad5*ΔKAN^r	This study
yDH354	*MATa BY4741 mre11*ΔKAN^r	This study
yDH355	*MATa BY4741 sgs1*ΔKAN^r	This study
yDH356	*MATa BY4741 esc2*ΔKAN^r	This study
yDH357	*MATa BY4741 xrs2*ΔKAN^r	This study
yDH358	*MATa BY4741 mms22*ΔKAN^r	This study
yDH359	*MATa BY4741 rad50*ΔKAN^r	This study
yDH360	*MATa BY4741 rtt101*ΔKAN^r	This study
yDH361	*MATa BY4741 rmi1*ΔKAN^r	This study
yDH362	*MATa BY4741 mms1*ΔKAN^r	This study
yDH363	*MATa BY4741 mms2*ΔKAN^r	This study
yDH399	*MATa BY4741 exo1*ΔKAN^r *pGAL-RAD18::HIS3MX6*	This study

[a] The wild-type strain is BY4741 (S288C). All the other strains are derived from BY4741.

For gene disruptions utilizing the *NATMX* or *HIS3MX* cassette, the *xxx*Δ::*KANMX* strain from the deletion array was converted to *xxx*Δ::*NATMX* or *xxx*Δ::*HIS3MX*. The cassette conversion was achieved by amplifying the *NATMX* or *HIS3MX* cassette with primers MX-F (5′-ACATGGAGGCCCAGAATACCCT-3′) and MX-R (5′-CAGTATAGCGACCAGCATTCAC-3′) from plasmids p4339 and pFA6a-His3MX6-pGAL1, respectively (17, 19), and the resulting PCR product was used to transform the *xxx*Δ::*KANMX* strain (the *-MX* cassettes each carry an identical 5′ TEF promoter and 3′ terminator, which facilitates the *KANMX*::*NATMX* or *KANMX*::*HISMX* conversion).

In order to integrate the *pGAL1* promoter into the −1 position of the *RAD18* and *RAD57* genes, a region of plasmid pFA6a-His3MX6-pGAL1 was amplified by PCR using primers that contain 55 bp of *RAD18* or *RAD57* gene sequence (−55 to −1 and +1 to +55), followed by 20 bp homologous to pFA6a-His3MX6-pGAL1 (17). The PCR product was used to transform the indicated target yeast strains and replaced the endogenous *RAD18* or *RAD57* promoter with the *pGAL1* promoter and *HIS3MX* marker. For *pGAL-RAD18*, the primers used were 5′AAACCATCCGCAAGTGAGCATCACAGCTACTAAGAAAAGGCCATTTTTACTACTCGAATTCGAGCTCGTTTAAAC-3′ and 5′-CAGGCTCGGTATTGAAGTAGTCGTGAAGTCGCTTGCAGTGGTTATTTGGTGGTCCATTTGAGATCCGGGTTTT-3′, and for *pGAL-RAD57*, the primers used were 5′-ATGAAAATGATGAACAACCACTGGGAATTCACCATTTTTCAAAGTGTGTAAATTCGAATTCGAGCTCGTTTAAAC-3′ and 5′-TTCATCGTAAAGGTCCATATACGTATTGTCAAATTTTATTGATAAGGCCCTAGGCATTTTGAGATCCGGGTTTT-3′.

Genome-wide low-dose sensitivity screen. The deletion array of ~4,700 viable yeast single-gene knockout strains (Open Biosystems) was replica pinned onto YPD and YPD plus 0.001% MMS plates using a 384-floating-pin replicator (V&P Scientific Inc.). The plates were incubated at

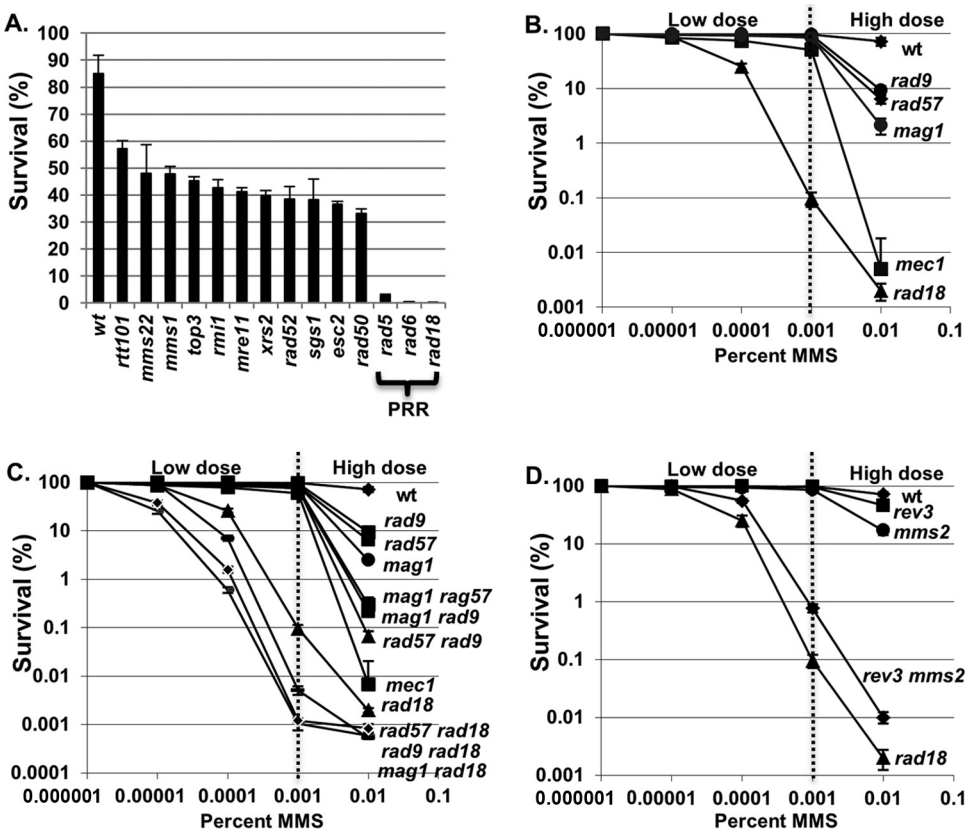

FIG 1 Postreplication repair pathways are required for survival in low-dose MMS. (A) Reconfirmed low-dose sensitivity mutants. Reconstructed yeast deletion mutants were grown to log phase in YPD medium with 0.001% MMS. Cells were taken out after 5 h of incubation at 30°C. Viable cells were determined by the number of CFU on YPD plates after 3 days of incubation at 30°C. Three independent transformants of each strain were tested, and the error bars indicate the standard deviations of viability measurements. wt, wild type. (B) Survival of a *rad18*Δ mutant strain in low-dose MMS compared to other DDR mutants. A panel of yeast mutants was exposed to the indicated concentrations of MMS during log-phase growth. Cells were removed after 5 h of incubation at 30°C and spread onto YPD plates. Viable cells were determined by the number of CFU after 3 days of incubation at 30°C. Each kill curve represents the mean viability from three independent experiments, and the error bars represent the standard deviations of the mean. (C) Survival of *rad18*Δ in low-dose MMS in combination with other DDR mutants. The indicated yeast mutant strains were grown in YPD medium with or without the indicated concentrations of MMS. Cells were taken out after 5 h of incubation at 30°C and spread onto YPD plates. Viable cells were determined by the number of CFU after 3 days of incubation at 30°C. Each kill curve represents the mean of three independent experiments, and the error bars represent the standard deviations of the mean. (D) Either branch of PRR is sufficient for cell survival in low-dose MMS. Wild-type and PRR mutant strains were exposed in log phase to various concentrations of MMS for 5 h. Cells were removed after the exposure and plated on YPD plates for determination of the survival rate as described above. Each kill curve represents the mean viability from three independent experiments, and the error bars represent the standard deviations of the mean.

30°C for 24 h before being scored for growth. The screen was subsequently repeated to control for false positives. Of note, in the initial screen, a *rad18*Δ mutant was not sensitive to 0.001% MMS, while its partner, *rad6*Δ, exhibited strong MMS sensitivity. We independently constructed a *rad18*Δ::*KANMX* gene knockout in a wild-type (BY4741) background, as described above. This newly constructed strain exhibited strong sensitivity to 0.001% MMS (identical to that of *rad6*Δ) (Fig. 1), leading us to believe that our original *rad18*Δ::*KANMX* library strain was of incorrect genotype or harbored a suppressor mutation. For follow-up studies, we used the newly constructed *rad18*Δ.

MMS kill curves. Cells (5×10^7) were harvested from log-phase cultures and resuspended in 10 ml fresh YPD medium with or without MMS (prepared from a master batch of YPD or YPD plus MMS). In order to reduce variability due to the extremely low doses examined in this study, a fresh master mix of 0.1% MMS in YPD medium was prepared, and lower concentrations were achieved by further diluting a proportion of the master mix with YPD. Following the addition of MMS, cultures were incubated at 30°C, and aliquots were taken out after 5 h of incubation (for MMS concentration-dependent kill curves) or at given intervals (for time course experiments). The cells were resuspended in PBS plus 5% sodium thiosulfate (to inactivate the MMS). The cells were sonicated, and cell concentrations were assessed using a Coulter Counter. Viability was determined by plating serial dilutions of cultures onto YPD (or YPG) plates and scoring the number of CFU after 3 to 4 days at 30°C. Viability was calculated as CFU/total cells.

Calculation of MMS-induced mutation frequency. The mutation frequency due to MMS treatment was measured by selection for canavanine resistance (due to forward mutation of the *CAN1* gene) after MMS treatment. Log-phase cells were exposed to MMS in liquid cultures for 5 h at 30°C as described above. Following MMS treatment, the cells were resuspended in PBS plus 5% sodium thiosulfate and subsequently serially diluted and plated onto synthetic defined medium (SD)-Arg-Ser plus 60 mg/liter canavanine (for the measurement of mutation rates) and YPD medium (for viability measurements). The plates were incubated at 30°C for 3 days, and mutations were assessed as the number of CFU on canavanine plates. MMS-induced mutation rates were determined by subtracting the number of mutations observed for cells without MMS treatment. Mutation rates are expressed as the number of canavanine-resistant cells per 10^6 viable cells.

Synchronization and cell cycle analysis. Cells were synchronized in the G_1 phase by the addition of α-factor (Zymo Research; catalog number Y1001) at a final concentration of 5 μM to log-phase cultures or cultures released from G_2 arrest (see below). Cultures were incubated in α-factor for 2 to 3 h at 30°C to achieve G_1 arrest, which was verified microscopically and by fluorescence-activated cell sorter (FACS) analysis. To release cells from G_1 arrest, cells were harvested and washed once with 1 ml of phosphate-buffered saline (PBS) and resuspended in 10 ml fresh YPD medium containing 10 μg/ml pronase (Fisher Scientific; catalog number 50-720-3354). For G_2/M synchronization, 10 μg/ml of nocodazole (Toronto Research Chemicals Inc.; catalog number M330350) was added to log-phase cultures or cultures released from G_1 arrest, and the cells were incubated for 2 h at 30°C. G_2-arrested cells were verified microscopically (as large-budded cells) and by FACS analysis. Cell cycle distributions were determined by flow cytometry (by a method described previously [20]) using a Beckman-Dickson FACSCalibur flow cytometer.

Western blotting. Cell extracts were prepared from log-phase cells, as well as synchronized cells, using a trichloroacetic acid (TCA) lysis method (21). Proteins were analyzed by SDS-PAGE (22). Rad53p was detected with the yC-19 anti-Rad53 antibody (Santa Cruz).

PFGE. To analyze intact yeast chromosomal DNA by pulsed-field gel electrophoresis (PFGE), DNA plugs were prepared using a CHEF (contour-clamped homogeneous electric field) Genomic DNA plug Kit (Bio-Rad; catalog number 170-3591) according to the manufacturer's instructions. Briefly, cells ($\sim 2 \times 10^8$) were harvested at different time points and fixed in 70% ethanol. Following ethanol fixation, the cells were resuspended in 200 μl of suspension buffer (10 mM Tris, pH 7.2, 20 mM NaCl, 50 mM EDTA) and mixed with an equal volume of 2% CleanCut low-melting-point agarose at 50°C. The hot mixture was quickly pipetted into the manufacturer-supplied plug molds and allowed to solidify (each sample produced 3 plugs). In-gel cell lysis was performed by adding lyticase (1 mg/ml) for 2 h at 37°C, followed by 1 mg/ml proteinase K treatment for 24 h at 37°C. In order to test whether the nondenatured DNA sample contained S1-labile ssDNA, a subset of the DNA plugs were digested with 1 U of S1 nuclease (Sigma; catalog number N5661) for 40 min at 30°C in S1 nuclease buffer containing 1 mM phenylmethylsulfonyl fluoride (PMSF) (the undigested set was incubated in the same buffer without S1 nuclease). Both sets of plugs were then loaded on a 1% Megabase agarose gel (Bio-Rad), and genomic DNA was resolved using a Bio-Rad CHEF-DR II system according to the manufacturer's instructions. Following electrophoresis, the gels were stained in 1% ethidium bromide for 2 h and photographed under UV light.

RESULTS

Postreplication repair is required for survival in response to continuous low-dose MMS exposure. While a genome-wide screen for mutants sensitive to high doses of MMS (0.035%) previously identified 103 sensitive mutant strains (23), we hypothesized that a different spectrum of mutants would be sensitive to low-dose MMS (0.001%). To test this hypothesis, we screened ~4,700 unique gene deletion strains representing the yeast haploid deletion collection (24) for mutations conferring sensitivity to 0.001% MMS. As a small percentage of the library strains have been shown to harbor additional mutations (25, 26), we sought to eliminate any false positives by regenerating all 14 deletion mutants that showed low-dose MMS sensitivity in the initial screen (see Materials and Methods). These new deletion mutants were then retested by quantitative colony-forming assay in response to MMS, and all 14 mutants were confirmed to be sensitive to 0.001% MMS (Fig. 1A). Mutations in the PRR genes *rad5*Δ, *rad6*Δ, and *rad18*Δ conferred particularly high (>100-fold) sensitivity, while the remaining mutants exhibited a milder 2- to 3-fold drop in survival. All of the genes identified as being sensitive to low-dose MMS had been previously identified as sensitive to high-dose MMS (23). To reconfirm that PRR mutants are unique among repair genes in their exquisite sensitivity to low-dose MMS, we performed a verification step in which we quantified the sensitivities of a panel of high-dose MMS-sensitive DDR mutants to a range of MMS exposures to confirm that they do not confer substantial sensitivity to low-dose MMS. This panel comprised genes involved in homologous recombination (HR) (*rad57*Δ), base excision repair (BER) (*mag1*Δ), and checkpoint activation (*rad9*Δ and *mec1*Δ) (Fig. 1B). While a *rad18*Δ mutant exhibited a drop in viability in MMS in a dose-dependent manner down to 0.0001% MMS, none of the other mutants exhibited substantial sensitivity to very low-dose MMS, despite significant sensitivity to high-dose (0.01%) treatment. From these results, we conclude that PRR mutants are highly sensitive to low-dose MMS treatment, whereas mutations in other DNA repair pathways (HR, BER, etc.) show minimal effect. Although the other pathways tested (HR, BER, etc.) are far less critical than PRR under low-dose conditions (i.e., ≤0.001% MMS), combining *rad18*Δ with mutations in *rad57*Δ, *rad9*Δ, or *mag1*Δ resulted in an additive increase in sensitivity to low-dose MMS versus *rad18*Δ alone (Fig. 1C), demonstrating that in the absence of *RAD18* these pathways play a compensatory role.

Either PRR subpathway (error free or error prone) is sufficient for survival in response to low-dose MMS. Cells employ two *RAD18*-dependent PRR mechanisms to tolerate DNA lesions (translesion synthesis and error-free HR-directed bypass). To determine whether *RAD18*-dependent survival in low-dose MMS depends on one or both of these mechanisms, we examined the low-dose MMS sensitivities of representative mutants for each PRR subpathway (*REV3*, which is required for translesion synthesis, and *MMS2*, which is required for error-free PRR [8, 27]). As shown in Fig. 1D, a defect in either PRR subpathway alone (*rev3*Δ or *mms2*Δ) does not affect survival in MMS concentrations of ≤0.001%, while both exhibit sensitivity to high-dose (0.01%) MMS (with *mms2*Δ exhibiting slightly higher sensitivity at this dose). In contrast, loss of both branches (*mms2*Δ *rev3*Δ) results in synergistic hypersensitivity to low-dose MMS (Fig. 1D). Thus, we conclude that either PRR subpathway (error free or error prone) is sufficient for survival in response to low-dose MMS. Notably, the *mms2*Δ *rev3*Δ double mutant is slightly more MMS resistant than a *rad18*Δ strain, suggesting that there is some remaining PRR activity in *mms2*Δ *rev3*Δ (possibly through a Rev1-Rad30-dependent translesion synthesis mechanism) (27, 28).

A G_2/M (but not intra-S) checkpoint is activated in PRR-deficient cells in low-dose MMS. As discussed above, wild-type cells exhibit minimal checkpoint activity in low-dose MMS. However, given the extremely low survival rate of PRR-defective *rad18*Δ cells in low-dose MMS, we hypothesized that the absence of PRR would cause a defect in replication fork progression and possibly activate the intra-S-phase checkpoint (29–31). To test this hypothesis, wild-type and *rad18*Δ cells were synchronized into the G_1 phase with α-factor and released into growth medium containing 0.001% MMS. Wild-type cells completed S phase within 30 to 40 min in the presence or absence of low-dose MMS and progressed through G_2/M, as seen by both flow cytometry and the budding index (Fig. 2A). Unexpectedly, MMS-treated *rad18*Δ cells progressed through S phase with kinetics similar to those of wild-type cells and subsequently arrested with 2C DNA content (Fig. 2A), with more than 80% exhibiting a large-budded morphology, which persisted for the duration of the experiment (180

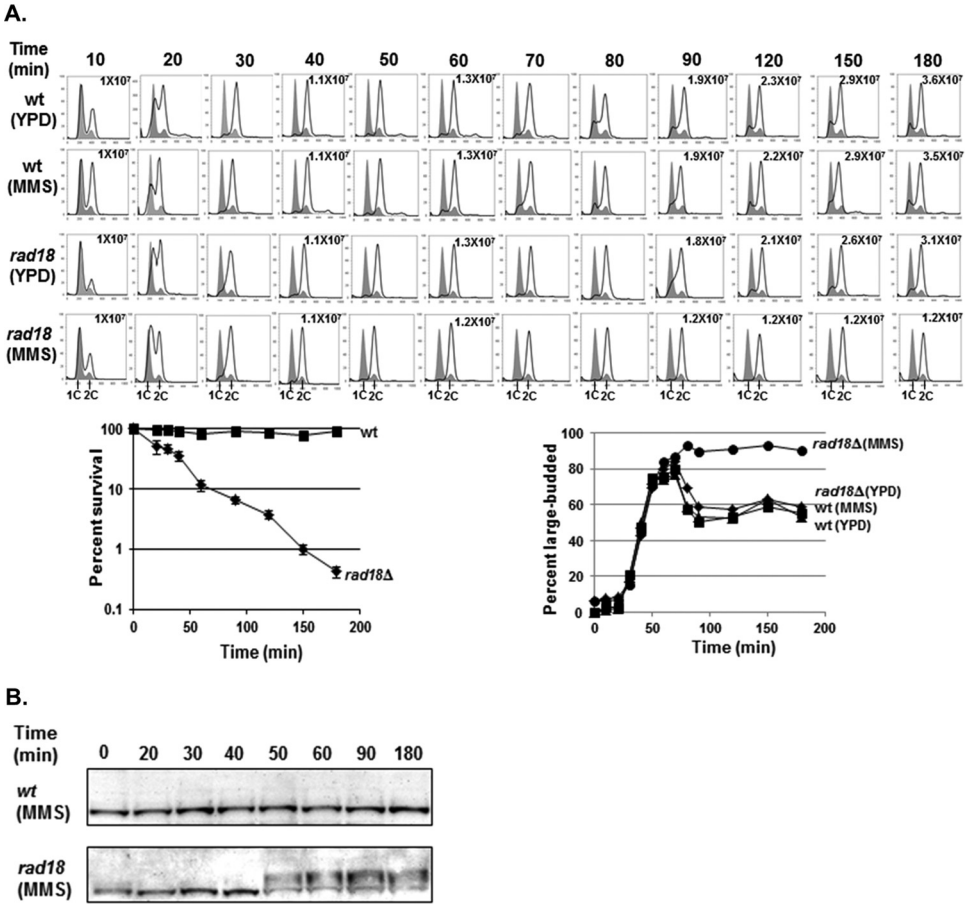

FIG 2 Low-dose MMS activates the G_2/M checkpoint in *rad18*Δ cells. (A) Low-dose MMS triggers G_2/M arrest in *rad18*Δ cells. Wild-type and *rad18*Δ cells were synchronized with α-factor and released into YPD medium ± 0.001% MMS. Cells were removed at the indicated times and analyzed for cell cycle distribution by FACS, for cell morphology by microscopy, and for viability by colony survival assay. Each flow cytometry graph contains two histograms. The shaded histograms represent the cell cycle distribution of α-factor-blocked cultures at time zero. The overlaid histograms represent the cell cycle distributions at various times following release from the G_1 block. The cell number per milliliter is listed for selected time points. Survival curves for wild-type and *rad18*Δ cells at each time point are shown below the cell cycle distribution graphs. Each strain was tested in triplicate, and the error bars represent the standard deviations of mean cell viability. (B) Rad53 phosphorylation in response to 0.001% MMS. Wild-type and *rad18*Δ cells were treated with α-factor and released into YPD medium with 0.001% MMS. Samples were taken out at the indicated times for Western blot analysis with an anti-Rad53 antibody.

min). Thus, *rad18*Δ cells arrest in G_2 phase after exposure to low-dose MMS but do not experience the significant S-phase delay indicative of intra-S-phase checkpoint activation (20, 31).

To confirm that the G_2 arrest of *rad18*Δ cells in low-dose MMS was due to the activation of the G_2/M DNA damage checkpoint, we tested for MMS-induced Rad53 phosphorylation (a G_2/M checkpoint indicator) by Western blotting (21). Indeed, while wild-type cells exhibited no Rad53 phosphorylation in low-dose MMS (consistent with no MMS-dependent changes in cell cycle distribution by FACS), *rad18*Δ cells exhibited Rad53 phosphorylation beginning at ~50 min after the addition of low-dose MMS (Fig. 2B). Of note, Rad53 phosphorylation in *rad18*Δ cells was somewhat delayed after the transition to 2C DNA content by FACS (Fig. 2A and B), suggesting that generating the checkpoint activation signal may require events that occur after the bulk of replication is completed.

Low-dose MMS-induced viability loss in *rad18*Δ cells requires passage through S phase in the presence of MMS. Given that the DDR checkpoint is not activated until after the bulk of replication has been completed, we hypothesized that the G_2/M arrest and the viability loss in *rad18*Δ cells exposed to low-dose MMS are not induced by alkylation lesions directly, but rather, by secondary lesions (such as ssDNA gaps) resulting from incomplete postreplication repair (32, 33). One prediction of this hypothesis is that *rad18*Δ cells exposed to low-dose MMS outside the S phase (i.e., in the G_1 or G_2 phase) should remain viable, since this would preclude the generation of irreparable PRR intermediates. To test this prediction, we induced a mitotic checkpoint arrest in wild-type and *rad18*Δ cells with nocodazole treatment and then released the cells into medium containing both 0.001% MMS and α-factor (to restrict MMS exposure to the G_1 phase). As expected, when the MMS treatment was confined to the G_1 phase (via α-factor treatment), *rad18*Δ cells exhibited significantly higher viability than cells allowed to replicate their genomes in the presence of MMS (no α-factor) (49% viable versus 3.5%) (Fig. 3A). (The ~50% drop in viability with α-factor likely reflects a subset of unrepaired lesions that persist after α-factor is removed; the cells are plated on YPD afterward, at which point they can cycle normally and must cope with any remaining MMS lesions). In conclusion, the MMS sensitivity exhibited by a *rad18*Δ mutant is due

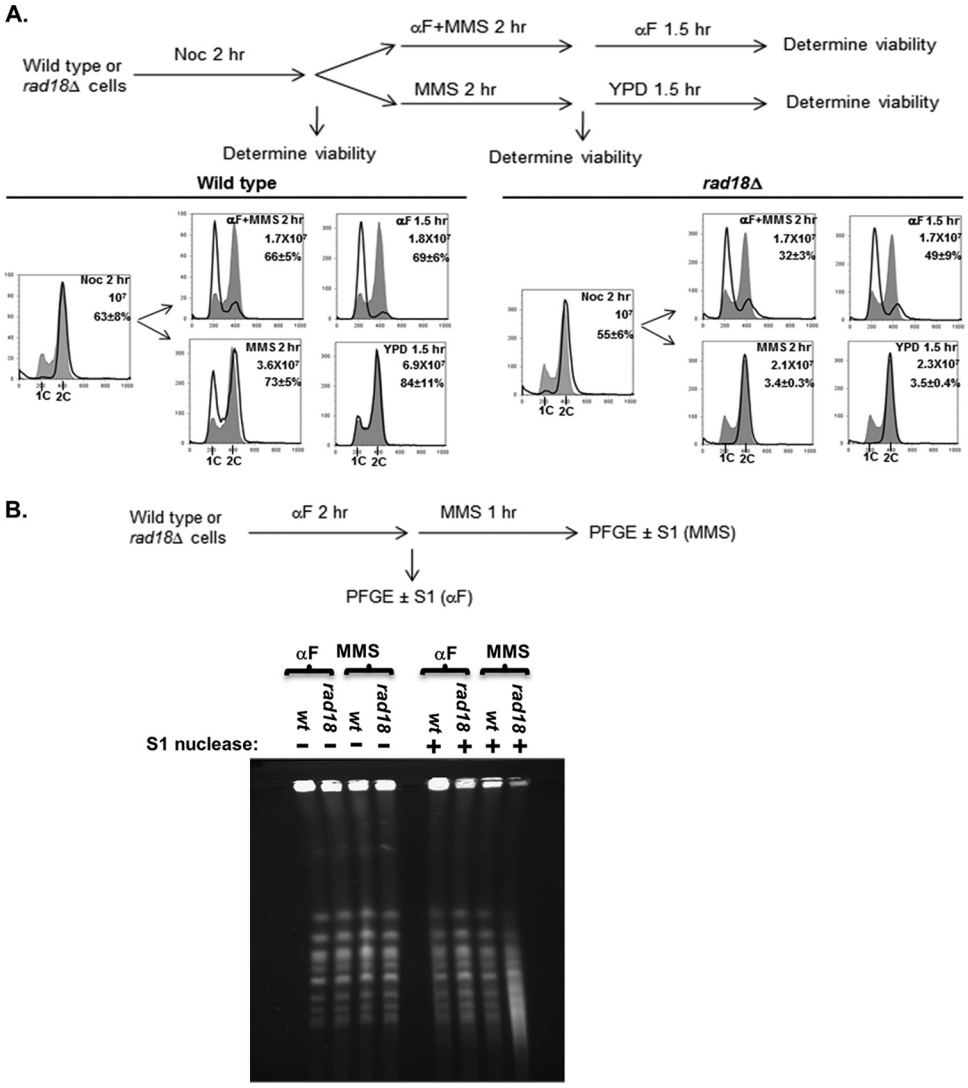

FIG 3 Loss of viability and G_2 arrest in *rad18*Δ cells in low-dose MMS is associated with S phase. (A) Passage through S phase is required for MMS sensitivity. Wild-type and *rad18*Δ cells were synchronized at mitotic checkpoint arrest with nocodazole (Noc) for 2 h and then exposed to 0.001% MMS in the presence or absence of α-factor for a second 2-h period. MMS was then removed, and the cells were incubated for another 1.5 h, with or without α-factor. Cells were withdrawn at the indicated time points for the assessment of cell cycle distributions and survival rates. All incubations occurred at 30°C. In the upper right corner of each graph are shown the duration of treatment, cell number per milliliter, and cell survival percentage at the end of each treatment (each strain was tested in triplicate repeats for survival rates; the mean and standard deviation of the mean survival rate are indicated). The shaded histograms represent the cell cycle distribution of the asynchronous culture before the nocodazole block. The overlaid histograms represent the cell cycle distributions at various times after release. (B) Chromosomes of MMS-treated *rad18*Δ cells show S1 nuclease-sensitive components (ssDNA gaps). α-Factor-blocked wild-type and *rad18*Δ cells were released into YPD medium with 0.001% MMS and 10 μg/ml nocodazole for 60 min. Cells were harvested after α-factor synchronization (αF) and after MMS treatment (MMS). Chromosomal DNA (either S1 treated or mock treated) was analyzed by PFGE.

to DNA damage produced during the S phase, likely caused by a defect in DNA damage tolerance during replication.

Previous reports have demonstrated that cells that enter S phase with irreparable UV lesions generate long stretches of ssDNA, and these ssDNA lesions are later resolved by postreplication repair (32, 33). We hypothesized that low-dose MMS treatment during S phase is also associated with the production of ssDNA gaps that are irreparable in a PRR mutant background (and cause the G_2 arrest). To test this hypothesis, we employed the single-strand-specific S1 endonuclease, which cuts DNA regions containing nicks and ssDNA gaps (34, 35), converting them into double-strand breaks (DSBs) that can be visualized as fragmentation by PFGE (36). Wild-type and *rad18*Δ cells were synchronized in the G_1 phase with α-factor and released into medium containing low-dose MMS (0.001%) plus nocodazole. (The nocodazole treatment was used to arrest wild-type cells at the mitotic checkpoint to minimize the ssDNA component associated with DNA replication and to make the results comparable to those for the G_2-arrested *rad18*Δ cells.) After a 60-min low-dose MMS treatment, chromosomal DNA was isolated in agarose plugs and subjected to S1 nuclease treatment and PFGE (Fig. 3B). For wild-type cells, treatment with low-dose MMS was not associated with detectable S1-dependent chromosomal fragmentation (and thus no ssDNA gaps). In contrast, *rad18*Δ cells exhibited significant

MMS- and S1-dependent chromosomal fragmentation that is indicative of the presence of ssDNA gaps associated with low-dose MMS exposure. From these data, we conclude that the loss of PRR is associated with the production of ssDNA gaps in low-dose MMS, and these lesions are the likely trigger for the prolonged checkpoint activation exhibited by these cells.

Both viability and chromosome integrity in low-dose MMS-treated *rad18*-deficient cells can be rescued in a time-limited fashion by reactivation of *RAD18* in G_2 phase. Recent work has shown that for acute high doses of UV and MMS, PRR can be delayed for a prolonged period past the completion of bulk DNA synthesis and then reactivated to restore a major proportion of cell viability (28, 37). As sensitivity to low-dose MMS for PRR mutants is associated with a prolonged G_2 checkpoint and ssDNA gaps, we hypothesized that reactivation of PRR in these cells would have a 3-fold effect: ssDNA gaps would be eliminated, cells would escape G_2 arrest, and viability would be restored. To test this hypothesis, we constructed a yeast strain harboring a *RAD18* gene under the control of a conditional *GAL* promoter (*GAL-RAD18*) to control the activity of PRR (28). Cells were exposed to low-dose MMS under *RAD18*-repressing conditions (i.e., glucose), and cells were withdrawn at multiple time points for assessment of viability on glucose plates (maintaining *RAD18* repression) and galactose plates (reactivating *RAD18*) (Fig. 4A). As expected, in glucose, cells harboring the *GAL-RAD18* construct exhibited prolonged low-dose MMS-dependent G_2 arrest (data not shown) and loss of viability, mimicking a *rad18*Δ deletion. However, when cells were removed and plated on galactose medium (reactivating *RAD18*) following MMS treatment, there was a marked increase in viability (nearly 100% rescue after up to 4 h in MMS). From these data, we conclude that the loss of viability in PRR-deficient cells in response to low-dose MMS treatment can be rescued by the reactivation of *RAD18*.

Notably, this rescue was evident even after prolonged MMS treatment but began to steadily decrease after the 4-h time point, and no rescue was observed after 8 h in low-dose MMS. We initially hypothesized that the failure to rescue at later time points was a result of new MMS lesions incurred during the prolonged exposure in G_2; however, even after removing the MMS after 3 h, *GAL-RAD18* cells remained arrested, and the galactose-dependent rescue was similarly time limited (data not shown). These data suggest that the loss of *RAD18*-dependent rescue after 8 h was not due to additional MMS lesions but to a secondary mechanism, possibly through further processing of ssDNA to a different lesion irreparable by PRR (32).

To confirm that the *RAD18*-dependent rescue in low-dose MMS correlates with a decrease in ssDNA gaps (indicative of repair by PRR), *GAL-RAD18* cells were exposed to low-dose MMS in glucose medium (*RAD18*-OFF) and then switched to either galactose medium (*RAD18*-ON) or fresh glucose medium in the presence of nocodazole. DNA samples were prepared in agarose plugs and subjected to S1 nuclease digestion and PFGE. As previously observed for *rad18*Δ (Fig. 3B), low-dose MMS-treated *GAL-RAD18* cells in glucose medium exhibited significant S1-dependent chromosomal fragmentation (Fig. 4B). However, when cells were switched to galactose medium (reactivating *RAD18*), a significant reduction in S1 nuclease sensitivity was observed, indicative of the restoration of ssDNA gaps to dsDNA by PRR. From these data, we conclude that the reactivation of *RAD18* after exposure to low-dose MMS is associated with the repair of ssDNA gaps and restoration of cell viability.

The time limit for *RAD18*-dependent rescue in low-dose MMS is *EXO1* dependent. While the reactivation of *GAL-RAD18* restores cell viability in low-dose MMS even after an extended delay (Fig. 4A), we were surprised that the ability to rescue was time limited. It has been previously reported that Exo1 possesses 5′-3′ exonuclease activity, and its processing of NER intermediates generates extended ssDNA gaps (38). We hypothesized that Exo1 enlarges ssDNA gaps in low-dose MMS during the prolonged G_2 arrest (either by a direct resection of the S-phase-dependent ssDNA or by extending new NER ssDNA intermediates that merge with the S-phase-dependent gaps) and that these extended gaps may be irreparable by PRR. This extension of ssDNA gaps into larger PRR-irreparable ssDNA regions could explain the inability to rescue low-dose MMS-treated *GAL-RAD18* cells past 8 h (Fig. 4A). To test this hypothesis, we deleted *EXO1* in a *GAL-RAD18* background and examined cell survival after prolonged incubation in low-dose MMS (Fig. 4C). Indeed, while the galactose-dependent *RAD18* rescue efficiency in an *exo1*Δ background was similar to that of *EXO1* at earlier time points, the ability to rescue cells by reactivation of *RAD18* in *exo1*Δ cells persisted well beyond 8 h. From this, we conclude that the time limit for *RAD18*-dependent rescue in low-dose MMS is due to *EXO1*-dependent resection. Interestingly, we observed a slight drop in rescue in an *exo1*Δ background (Fig. 4C), which may reflect the activities of other nucleases on ssDNA gaps.

Removal of the *SRS2*-dependent block to HR results in an efficient postreplicative rescue independent of *RAD18*. We were surprised that the extreme loss of viability in a *rad18*Δ mutant in low-dose MMS was due to the presence of ssDNA gaps, as it is unclear why these structures could not be repaired by sister chromatid recombination in the G_2 phase in a PRR-independent manner. We hypothesized that while it may be possible for these structures to be physically repaired by recombination, the repression of recombination by some unknown factor suppresses the repair. One candidate for this repression is the Srs2 helicase, which has been shown to suppress HR during DNA replication (39). Deletion of *SRS2* has been shown to rescue a *rad18*Δ mutant after low-dose UV treatment (40). We asked whether a similar effect may occur in low-dose MMS, and especially, whether delayed induction of HR at various time points during the low-dose MMS treatment may be sufficient to rescue *rad18*Δ cells in the absence of *SRS2*. In order to test this, we put *RAD57* under the control of a conditional *GAL* promoter and tested the effects of induction of *RAD57* on cell viability in a *rad18*Δ background. When *rad18*Δ *GAL-RAD57* and *srs2*Δ *rad18*Δ *GAL-RAD57* cells were exposed to low-dose MMS in glucose medium (*RAD57*-OFF), both strains exhibited viability loss and synchronization at G_2/M (Fig. 5A and data not shown). However, when MMS-treated *srs2*Δ *rad18*Δ *GAL-RAD57* cells were plated on galactose medium (reactivating *RAD57*), we observed a complete rescue of viability, indicating that in an *srs2*Δ background, HR can compensate for the loss of *RAD18*.

We note that even when *SRS2* is present, we observed a slight rescue upon reactivation of *GAL-RAD57* (Fig. 5A); this is likely due to *RAD57* overexpression, which may partially overcome *SRS2*-dependent inhibition (Rad57 can physically block Srs2's ability to disrupt Rad51 nucleoprotein filaments) (41). Interestingly, unlike the rescue by *GAL-RAD18*, the reactivation of *GAL-*

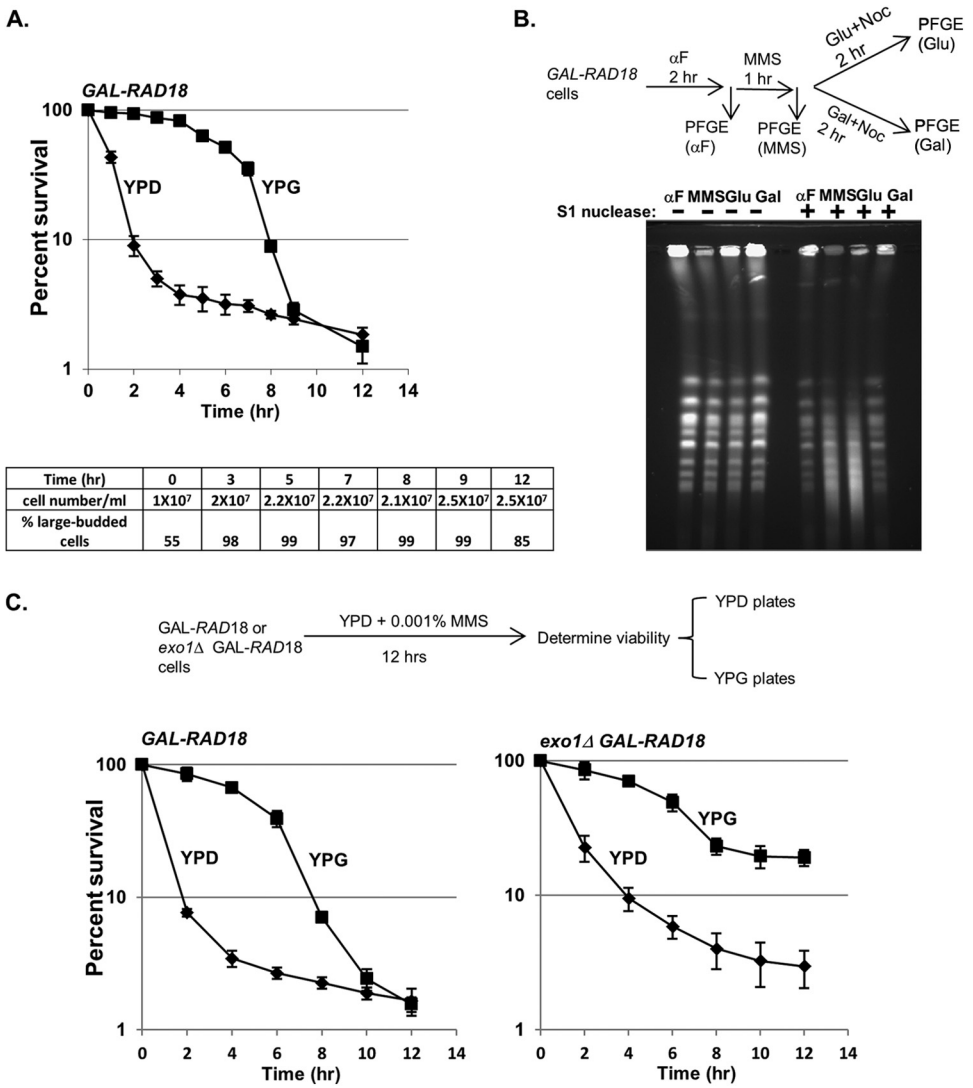

Time (hr)	0	3	5	7	8	9	12
cell number/ml	$1X10^7$	$2X10^7$	$2.2X10^7$	$2.2X10^7$	$2.1X10^7$	$2.5X10^7$	$2.5X10^7$
% large-budded cells	55	98	99	97	99	99	85

FIG 4 Reactivation of Rad18 in G_2 restores viability and chromosome integrity of low-dose MMS-treated *rad18* cells. (A) The viability of PRR-deficient cells can be restored when *RAD18* expression is induced after MMS treatment. Cells harboring a chromosomal *RAD18* gene under the control of a GAL promoter (GAL-*RAD18*) were grown in YPD medium with 0.001% MMS. At the indicated times of exposure, cells were withdrawn and analyzed for plating efficiency on either glucose or galactose plates. Each kill curve represents the mean viability of three independent experiments, and the error bars represent the standard deviations of the mean. At all time points after 2 h of exposure to MMS, the cell density remained essentially unchanged, and *rad18*Δ cells accumulated with a uniform large-budded morphology (bottom). (B) Induction of *RAD18* reduces S1 sensitivity in MMS-treated *GAL-RAD18* cells. *GAL-RAD18* cells were blocked with α-factor, released into YPD medium with 0.001% MMS for 60 min, and then incubated in MMS-free medium containing glucose or galactose for another 2 h in the presence of nocodazole (10 μg/ml). Cells were withdrawn after α-factor synchronization (αF) and MMS exposure and after the subsequent *RAD18* induction (Glu and Gal). Chromosomal DNA was treated with S1 nuclease or mock treated and subjected to PFGE as described for Fig. 3B. (C) The ability for *RAD18*-dependent rescue is prolonged in the absence of *EXO1*. *GAL-RAD18* and *exo1*Δ *GAL-RAD18* cells were grown in YPD with 0.001% MMS for a period of 12 h. The survival rates on glucose or galactose plates were determined as for panel A.

RAD57 allows rescue even after 8 h of MMS exposure (Fig. 5B), suggesting that the *EXO1*-dependent extension of ssDNA can be resolved by HR, but not PRR. From these data, we conclude that *SRS2* represses the HR-dependent repair of ssDNA gaps in PRR-deficient cells.

The preference for error-free and error-prone lesion tolerance is cell cycle dependent. Since *RAD18* is required for the function of either error-free or error-prone PRR, we next asked whether one pathway is more important for survival in low-dose MMS following the reactivation of *GAL-RAD18*. To determine this, we combined the conditional *GAL-RAD18* allele with deletions of either *rev3*Δ (TLS deficient) or *mms2*Δ (error-free-PRR deficient) and tested the abilities of these mutants to be rescued by induction of *GAL-RAD18* at various times during low-dose MMS treatment. While *GAL-RAD18* induction rescued the *mms2*Δ mutant, the efficiency of rescue by activation of *GAL-RAD18* in a *rev3*Δ background was markedly reduced (Fig. 6A), indicating that the postreplicative rescue in low-dose MMS depends on functional translesion synthesis. This is consistent with previous observations for UV lesion bypass (28).

Based on the importance of *REV3*-dependent, error-prone TLS for the rescue of GAL-*RAD18* cells, we predicted that the

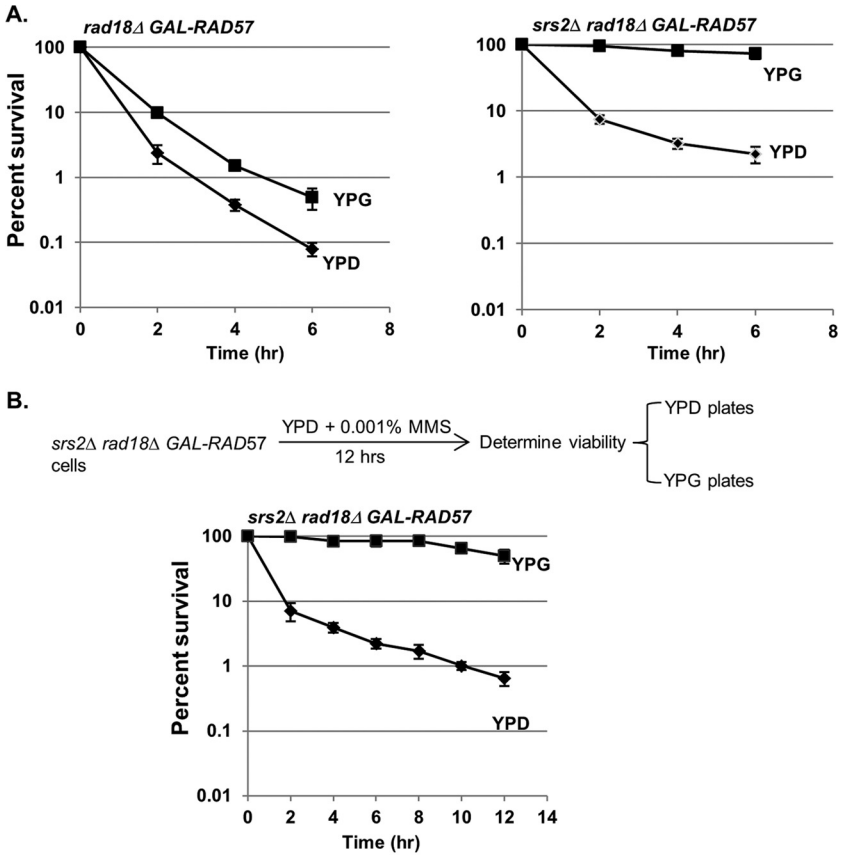

Time (hr)	0	2	4	6	8	10	12
cell number/ml	$7.8X10^6$	$1.4X10^7$	$1.6X10^7$	$1.8X10^7$	$1.9X10^7$	$2.2X10^7$	$2.3X10^7$
% large-budded cells	53	84	87	90	87	85	87

FIG 5 Rescue of *rad18*Δ cells by HR. (A) Induction of *RAD57* results in the rescue of viability in *rad18*Δ cells in the absence of *SRS2*. *rad18*Δ *GAL-RAD57* or *srs2*Δ *rad18*Δ *GAL-RAD57* cells were grown in YPD medium with 0.001% MMS. Kill curves were determined on glucose and galactose plates as described in the legend to Fig. 4A. Each strain was tested in triplicate repeats, and the error bars represent the standard deviations of mean viability. (B) *RAD57* induction rescues viability of *rad18*Δ cells in the absence of *SRS2* after prolonged incubation. *srs2*Δ *rad18*Δ *GAL-RAD18* cells were grown in YPD with 0.001% MMS over a prolonged period (12 h). Cells were withdrawn at the indicated exposure times and analyzed for cell density, cell morphology, and plating efficiency on either YPD or YPG (galactose) plates as described in the legend to Fig. 4A.

reactivation of *RAD18* in G_2 should cause hypermutability in low-dose MMS. To test this prediction, we determined mutation rates in *GAL-RAD18* cells after the induction of *RAD18* following exposure to low-dose MMS for 5 h. As predicted, *GAL-RAD18* cells show significantly elevated MMS-induced mutation rates in low-dose MMS after the induction of *RAD18* compared to wild-type cells (Fig. 6B); this hypermutability is dependent on *REV3* (Fig. 6B), further confirming that inducing PRR in G_2 favors error-prone translesion synthesis. Of note, the *GAL-RAD18* cells exhibited slightly increased mutagenesis relative to the wild type even in the absence of galactose; this likely reflects some low-level *RAD18* expression due to the leakiness associated with the GAL promoter. As a control, we also determined MMS-induced mutation rates in *srs2*Δ *rad18*Δ *GAL-RAD57* cells after *RAD57* induction. While induction of GAL-*RAD57* in G_2 rescues viability in an *srs2*Δ *rad18*Δ mutant (Fig. 5A), this rescue should involve an error-free mechanism and thus should not be associated with hypermutability. As predicted, in contrast to induction of *GAL-RAD18*, hyperactivation of HR after low-dose MMS exposure does not significantly increase the mutation rate (Fig. 6B), indicating that while HR promotes the survival of *rad18*Δ cells in low-dose MMS, this repair involves an error-free mechanism. From these data, we conclude that reactivation of *RAD18*-dependent PRR in G_2 favors the mutagenic translesion synthesis pathway.

Our finding that the error-prone translesion synthesis pathway clearly predominates when *RAD18* is reactivated in G_2 is surprising given previous results showing that the error-free pathway is normally the dominant form of PRR (4, 42). To explain this discrepancy, we hypothesized that the predominance of translesion synthesis may be specific to the G_2 phase, whereas the error-free pathway normally predominates in S phase. Based on this prediction, an error-free-defective *mms2*Δ strain should produce more ssDNA gaps than an error-prone-defective *rev3*Δ strain in low-dose MMS. To test this prediction, we synchronized wild-type, *rev3*Δ, and *mms2*Δ cells in G_1 and released them into growth medium containing 0.001% MMS. While *rev3*Δ cells showed cell cycle progression kinetics similar to those of wild-type cells in low-dose MMS, *mms2*Δ cells exhibited a significant delay in G_2 (30 min) (Fig. 6C). Although MMS-treated *mms2*Δ cells did not ex-

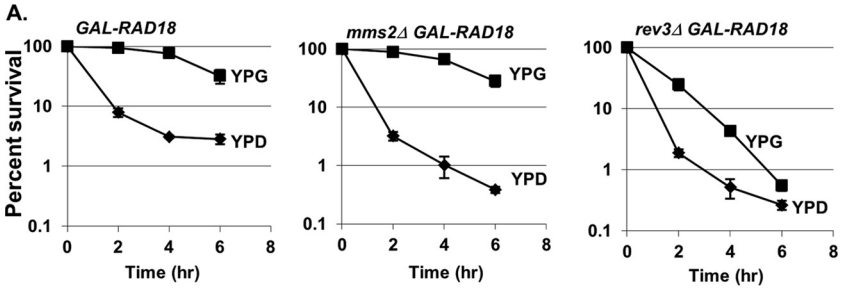
A.
GAL-RAD18
mms2Δ GAL-RAD18
rev3Δ GAL-RAD18
Percent survival
YPG
YPD
Time (hr)

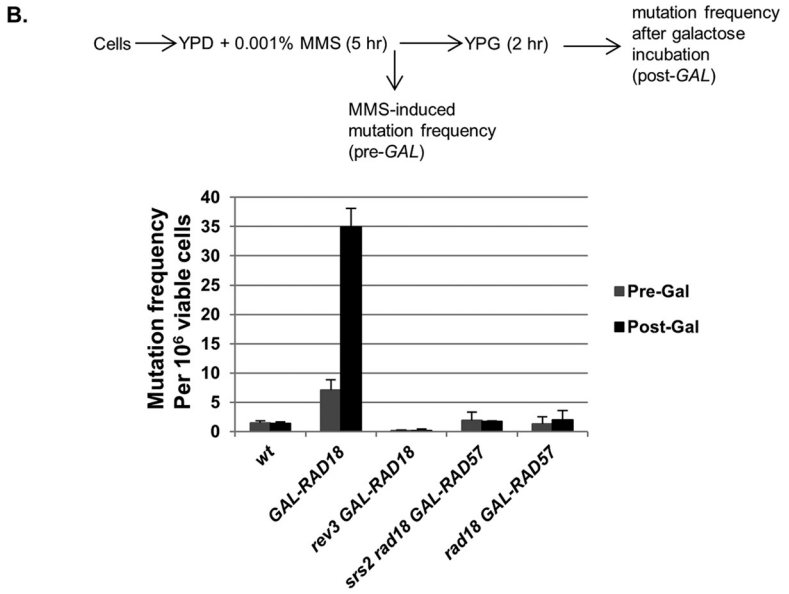
B.
Cells
YPD + 0.001% MMS (5 hr)
YPG (2 hr)
mutation frequency after galactose incubation (post-GAL)
MMS-induced mutation frequency (pre-GAL)
Mutation frequency Per 10^6 viable cells
Pre-Gal
Post-Gal
wt
GAL-RAD18
rev3 GAL-RAD18
srs2 rad18 GAL-RAD57
rad18 GAL-RAD57

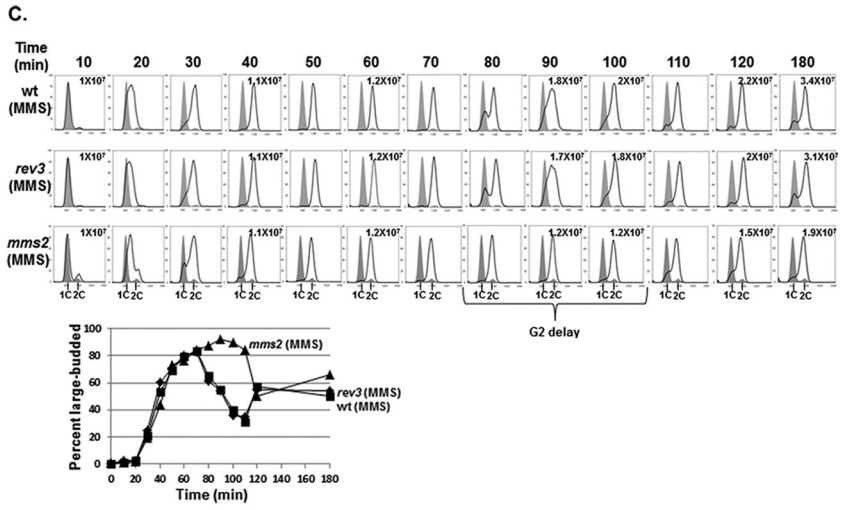
C.
Time (min)
wt (MMS)
rev3 (MMS)
mms2 (MMS)
G2 delay
Percent large-budded
Time (min)

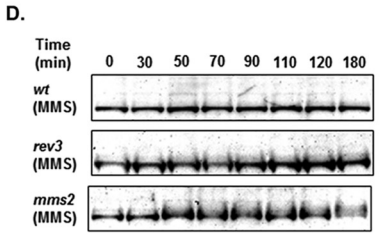
D.
Time (min)
wt (MMS)
rev3 (MMS)
mms2 (MMS)

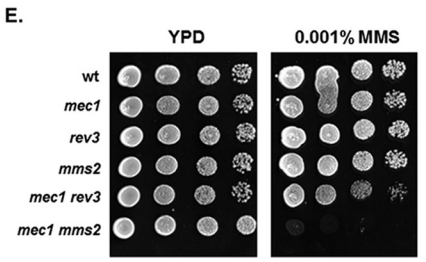
E.
YPD
0.001% MMS
wt
mec1
rev3
mms2
mec1 rev3
mec1 mms2

hibit substantially increased levels of Rad53 phosphorylation (Fig. 6D), we found that when *mms2*Δ is combined with deletion of the checkpoint factor *MEC1*, cells fail to grow in low-dose MMS (in contrast, a *rev3*Δ *mec1*Δ strain displays robust growth) (Fig. 6E). From these data, we conclude that loss of the *MMS2*-dependent error-free pathway is associated with a significant G_2 delay and a requirement for *MEC1* for survival in low-dose MMS, while loss of the *REV3*-dependent pathway does not exhibit these phenotypes.

DISCUSSION

Definition of "low-dose" treatment. Our motivation for providing a formal definition for what constitutes a "low dose" of a DNA-damaging agent stemmed from difficulties we experienced in comparing our data with other studies of low-level exposure that span a variety of dose rates, genotoxic agents, and cells/tissues. For example, in previous studies evaluating the role of PRR in response to low-dose UV treatment, Hishida et al. based their choice of UV irradiation dose (0.1 J/m^2/min) on the natural phenomenon (sunlight exposure) that they were attempting to mimic (4, 40); a clear analog for this dose using a chemical carcinogen such as MMS was not immediately apparent. By providing a physiological and agent-agnostic definition of "low-dose" DNA damage based upon the sensitivity of wild-type and mutant cells, we were able to reconcile our MMS results with these previous studies; both 0.1 J/m^2/min UV exposure and 0.001% MMS treatment fail to induce any discernible cellular sensitivity in a wild-type cell population; however, mutant studies reveal an exquisite and profound dependence on PRR for survival in response to low-dose damage (Fig. 1) (4).

PRR mutants are unique in their exquisite sensitivity to low-dose MMS. As the prior Hishida et al. study (4) was UV specific and screened only a small panel of known DDR targets, it remained formally possible that PRR reliance was UV specific or that other, unscreened genes would also be required for survival under low-dose conditions. To answer these questions, we performed a genome-wide screen in response to low-dose treatment with a DNA-alkylating agent (0.001% MMS). Strikingly, we show that while 0.001% MMS treatment of wild-type yeast cells produces no discernible response (for any assay by which we evaluate these cells, including survival [Fig. 1], checkpoint activity [Fig. 2], cell growth and division [Fig. 2], and chromosomal integrity/mutagenesis [Fig. 3B and 6B]), PRR mutants are exquisitely sensitive, and hence DNA damage tolerance is actively employed and critical for viability at this dose. The lethal lesions that render PRR mutants extremely MMS sensitive are unreplicated ssDNA gaps (which can be detected as S1-dependent fragmentation in *rad18* cells by PFGE [Fig. 3B]), and restoration of PRR activity (even after significant delay) eliminates these gaps and rescues cell viability in low-dose MMS (Fig. 4A to C). Due to the exceptional requirement for PRR under low-dose conditions, we were able to glean vital information regarding how PRR functions in the presence (or absence) of cell cycle checkpoints and how timing and context play vital roles in determining which PRR pathway (error free or error prone) is utilized.

The preference for error-free or error-prone PRR is cell cycle dependent. While previous studies have shown a cellular preference for the error-free pathway (4, 42), recent studies using an inducible PRR system show a clear preference for error-prone translesion synthesis (28). In this study, we show that these are not contradictory conclusions, since our data demonstrate that PRR pathway usage depends on timing and context. Specifically, while our data show a preference for the error-free pathway when cells are replicating in low-dose MMS, the error-prone pathway is specifically required for viability when PRR is delayed until the G_2 phase (Fig. 6A). These results provide some clarity with regard to how cells choose error-free versus error-prone repair (in low-dose MMS). During S phase, cells prevent ssDNA gap formation via the *MMS2*-dependent template switch mechanism (without requiring G_2 arrest) but, alternatively, can generate and repair an ssDNA gap using a *REV3*-dependent TLS mechanism (which can be delayed postreplication but requires checkpoint activation). The cell cycle dependence of error-free versus error-prone repair may reflect a necessity for template switching to happen within a brief window of lesion encounter by replicative polymerases, while TLS may be less temporally restricted. Alternatively, cells may directly regulate TLS or error-free factors in a cell cycle-dependent manner in order to carry out this programmed response. Consistent with this hypothesis, *REV1* expression peaks during the G_2 phase of the cell cycle; this transcriptional regulation may be one way in which cells suppress TLS in the S phase but promote it in G_2 (43).

Rescue by reactivation of PRR in MMS has a time limit. The inducible *GAL-RAD18* system also provides information on the stability of ssDNA lesions over a prolonged period. We show that there is a time limit for the delayed repair of ssDNA gaps in G_2/M; the reactivation of PRR is most effective within ~4 h after the initial G_2/M checkpoint activation (Fig. 4A); however, this time limit can be extended by deletion of the Exo1 exonuclease

FIG 6 TLS is required for the rescue of viability upon *RAD18* induction. (A) Reactivation of *RAD18* at G_2 fails to effectively rescue viability in the absence of *REV3*. *GAL-RAD18*, *rev3*Δ *GAL-RAD18*, and *mms2*Δ *GAL-RAD18* cells were exposed to 0.001% MMS over a 6-hour period. Cells were withdrawn at the indicated times during the exposure and analyzed for viability by plating efficiency on either glucose or galactose plates as described for Fig. 4A. Each strain was tested in triplicate repeats, and the error bars represent the standard deviations of the mean. (B) Reactivation of *RAD18* causes hypermutability. Log-phase wild-type, *GAL-RAD18*, or *GAL-RAD57* cells were grown in YPD with 0.001% MMS for 5 h and then incubated in fresh YPG medium for another 2 h. Cells were withdrawn before and after low-dose MMS treatment and before and after galactose incubation (Pre-Gal and Post-Gal) and assayed for viability and the induction of mutation to Can^r. Each strain was tested in triplicate repeats, and the error bars represent the standard deviations of mean viability. (C) *mms2*Δ cells show a G_2 delay in low-dose MMS. Wild-type, *rev3*Δ, and *mms2*Δ cells were synchronized in G_1 with α-factor and released into YPD medium with 0.001% MMS. Cells were removed at the indicated times and analyzed for cell cycle distribution by FACS and for cell morphology by microscopy. Each graph contains two histograms. The shaded histograms represent the cell cycle distribution of α-factor-blocked cultures at time zero. The overlaid histograms represent the cell cycle distribution at the indicated times following release. The cell density in cells per milliliter is listed for selected time points. (D) Detection of Rad53 phosphorylation in wild-type, *mms2*Δ, and *rev3*Δ cells in response to 0.001% MMS. Wild-type, *rev3*Δ, and *mms2*Δ cells were treated with α-factor and released into YPD medium with 0.001% MMS. Samples were taken out at the indicated times for Western blot analysis with an anti-Rad53 antibody. (E) Interactions between *mec1* and PRR mutants in low-dose MMS. The wild type and the indicated mutant strains were grown in YPD to saturation overnight at 30°C. Serial 10-fold dilutions were spotted onto YPD and YPD plus 0.001% MMS plates. (The *mec1*Δ strain is *sml1*Δ *mec1*Δ. The *sml1*Δ single mutation does not affect growth or survival at the tested MMS concentrations [data not shown]).

(Fig. 4C). From these data, we hypothesize that *EXO1*-associated extension of ssDNA gaps leads to large regions of ssDNA that are irreparable by *REV3*-dependent translesion synthesis. There are multiple possible mechanisms. For example, Exo1 could perform end resection directly on the ssDNA-dsDNA junctions at the end of each gap, similar to its role in resection of NER intermediates (38). Alternatively, this gap extension may be due to Exo1's known role in the extension of NER intermediates, and the resection of NER intermediates may encroach upon and merge with nearby ssDNA gaps. While Rev3 is known to be a low-processivity polymerase (44), it is not yet known on how large an ssDNA region Rev3 can act. One possible scenario is that following reactivation of PRR by *GAL-RAD18*, translesion synthesis must act to fill in ssDNA gaps prior to checkpoint adaptation (45), and further *EXO1*-dependent resection at later time points coupled with a low-processivity Rev3 polymerase may cause adaptation to outpace translesion synthesis (resulting in the segregation of incompletely replicated chromosomes). Thus, the multiple-hour delay before *rad18*-dependent ssDNA gaps become irreparable may be due to a low processivity rate for Exo1 at ssDNA gaps or may reflect an inability to maintain repression of Exo1 over prolonged periods (45, 46).

An additional question to be considered is why the Exo1-mediated ssDNA gaps are lethal to *rad18* cells (which presumably have an active HR pathway). In their low-dose UV studies, Hishida et al. discovered that the UV sensitivity of *rad18* cells can be suppressed by deleting the HR inhibitor *SRS2* (40). We extend this to show that the inability to repair ssDNA gaps by HR in *rad18* cells is due to an *SRS2*-dependent block; deletion of *SRS2* rescues viability in *rad18* cells only when HR is active (via *GAL-RAD57*) (Fig. 5). Intriguingly, the *srs2*-dependent repair is not time limited, unlike *EXO1*-dependent TLS repair of ssDNA gaps (Fig. 4). Thus, the question remains why the Srs2 HR block persists, as ssDNA gaps are repairable in its absence. We propose that the repression of HR by Srs2 at ssDNA may be initiated in an irreversible manner at a specific point in the cell cycle (possibly coincidental with the passage of the replication fork); hence, following ssDNA gap formation (a precursor to TLS repair), the option to utilize homologous recombination may no longer be available.

The low-dose hypermutability challenges our assumptions of what is a "safe dose." In this study, we describe the treatment of yeast cells with extremely low doses of MMS (from 0.001% to 0.0001%), which for normal cells do not induce any discernible phenotypes and yet are catastrophic for PRR mutants. Despite this, in the absence of any exogenous damage, a *rad18*Δ mutant exhibits growth characteristics that are similar to those of a wild-type cell. Applying this concept to the human condition raises important issues with regard to how we evaluate "safe" levels of carcinogenic substances. What might represent a negligible level for one person may result in significant unrepaired DNA damage for a second individual (such as someone who carries one or more mutations in PRR genes). While low-dose X rays have been a mainstay of diagnostic medical and dental procedures for decades and have recently become ubiquitous in airport security measures (47–49), estimations of the cancer risk associated with these sources are extrapolated from studies involving subjects who have encountered significantly higher doses (i.e., nuclear accident victims and atomic bomb survivors), largely ignoring individual genetic risk (49–54). Underestimating the carcinogenic potential of low-dose DNA damage is of critical importance, as evidenced by recent studies showing increased risks for malignancy related to radiation exposure from medical procedures (47, 48, 55, 56). An interesting question is whether we could identify at-risk individuals based upon their cellular proficiency in the low-dose (i.e., PRR-dependent) DNA damage response.

ACKNOWLEDGMENTS

We thank Brenda Andrews and Charles Boone for strains and plasmids used in this study and anonymous reviewers for helpful suggestions.

B.D.P. was supported by a U.S. Department of Defense Breast Cancer Research Program predoctoral fellowship. This work was supported by NIH grant R01 CA 129604.

REFERENCES

1. **Lazzaro F, Giannattasio M, Puddu F, Granata M, Pellicioli A, Plevani P, Muzi-Falconi M.** 2009. Checkpoint mechanisms at the intersection between DNA damage and repair. DNA Repair **8**:1055–1067.
2. **Drabløs F, Feyzi E, Aas PA, Vaagbø CB, Kavli B, Bratlie MS, Peña-Diaz J, Otterlei M, Slupphaug G, Krokan HE.** 2004. Alkylation damage in DNA and RNA-repair mechanisms and medical significance. DNA Repair **3**:1389–1407.
3. **Lindahl T.** 1993. Instability and decay of the primary structure of DNA. Nature **362**:709–715.
4. **Hishida T, Kubota Y, Carr AM, Iwasaki H.** 2009. *RAD6-RAD18-RAD5*-pathway-dependent tolerance to chronic low-dose ultraviolet light. Nature **457**:612–615.
5. **Tercero JA, Longhese MP, Diffley JF.** 2003. A central role for DNA replication forks in checkpoint activation and response. Mol. Cell **11**:1323–1336.
6. **Murakami-Sekimata A, Huang D, Piening BD, Bangur C, Paulovich AG.** 2010. The *Saccharomyces cerevisiae RAD9*, *RAD17* and *RAD24* genes are required for suppression of mutagenic post-replicative repair during chronic DNA damage. DNA Repair **9**:824–834.
7. **Shulman LN.** 1993. The biology of alkylating-agent cellular injury. Hematol. Oncol. Clin. North Am. **7**:325–335.
8. **Broomfield S, Chow BL, Xiao W.** 1998. MMS2, encoding an ubiquitin-conjugating-enzyme-like protein, is a member of the yeast error-free postreplication repair pathway. Proc. Natl. Acad. Sci. U. S. A. **95**:5678–5683.
9. **Prakash L, Prakash S.** 1977. Isolation and characterization of MMS-sensitive mutants of Saccharomyces cerevisiae. Genetics **86**:33–55.
10. **Prakash S, Prakash L.** 1977. Increased spontaneous mitotic segregation in MMS-sensitive mutants of Saccharomyces cerevisiae. Genetics **87**:229–236.
11. **Tercero JA, Diffley JF.** 2001. Regulation of DNA replication fork progression through damaged DNA by the Mec1/Rad53 checkpoint. Nature **412**:553–557.
12. **Andersen PL, Xu F, Xiao W.** 2008. Eukaryotic DNA damage tolerance and translesion synthesis through covalent modifications of PCNA. Cell Res. **18**:162–173.
13. **Ulrich HD, Walden H.** 2010. Ubiquitin signaling in DNA replication and repair. Nat. Rev. Mol. Cell Biol. **11**:479–489.
14. **Ulrich HD.** 2011. Timing and spacing of ubiquitin-dependent DNA damage bypass. FEBS Lett. **585**:2861–2867.
15. **Nelson JR, Lawrence CW, Hinkle DC.** 1996. Thymine-thymine dimer bypass by yeast DNA polymerase zeta. Science **272**:1646–1649.
16. **Blastyák A, Pintér L, Unk I, Prakash L, Prakash S, Haracska L.** 2007. Yeast Rad5 protein required for postreplication repair has a DNA helicase activity specific for replication fork regression. Mol. Cell **28**:167–175.
17. **Longtine MS, McKenzie A, III, Demarini DJ, Shah NG, Wach A, Brachat A, Philippsen P, Pringle JR.** 1998. Additional modules for versatile and economical PCR-based gene deletion and modification in Saccharomyces cerevisiae. Yeast **14**:953–961.
18. **Reid RJD, Sunjevaric I, Keddache M, Rothstein R.** 2002. Efficient PCR-based gene disruption in *Saccharomyces* strains using intergenic primers. Yeast **19**:319–328.
19. **Tong AH, Boone C.** 2006. Synthetic genetic array analysis in Saccharomyces cerevisiae. Methods Mol. Biol. **313**:171–192.
20. **Paulovich AG, Margulies RU, Garvik BM, Hartwell LH.** 1997. RAD9, RAD17, and RAD24 are required for S phase regulation in Saccharomyces cerevisiae in response to DNA damage. Genetics **145**:45–62.

21. **Pellicioli A, Lucca C, Liberi G, Marini F, Lopes M, Plevani P, Romano A, Di Fiore PP, Foiani M.** 1999. Activation of Rad53 kinase in response to DNA damage and its effect in modulating phosphorylation of the lagging strand DNA polymerase. EMBO J. **18**:6561–6572.
22. **Laemmli UK.** 1970. Cleavage of structural proteins during the assembly of the head of bacteriophage T4. Nature **227**:680–685.
23. **Chang M, Bellaoui M, Boone C, Brown GW.** 2002. A genome-wide screen for methyl methanesulfonate-sensitive mutants reveals genes required for S phase progression in the presence of DNA damage. Proc. Natl. Acad. Sci. U. S. A. **99**:16934–16939.
24. **Winzeler EA, Shoemaker DD, Astromoff A, Liang H, Anderson K, Andre B, Bangham R, Benito R, Boeke JD, Bussey H, Chu AM, Connelly C, Davis K, Dietrich F, Dow SW, El Bakkoury M, Foury F, Friend SH, Gentalen E, Giaever G, Hegemann JH, Jones T, Laub M, Liao H, Liebundguth N, Lockhart DJ, Lucau-Danila A, Lussier M, M'Rabet N, Menard P, Mittmann M, Pai C, Rebischung C, Revuelta JL, Riles L, Roberts CJ, Ross-MacDonald P, Scherens B, Snyder M, Sookhai-Mahadeo S, Storms RK, Véronneau S, Voet M, Volckaert G, Ward TR, Wysocki R, Yen GS, Yu K, Zimmermann K, Philippsen P, Johnston M, Davis RW.** 1999. Functional characterization of the *Saccharomyces cerevisiae* genome by gene deletion and parallel analysis. Science **285**:901–906.
25. **Grunenfelder B, Winzeler EA.** 2002. Treasures and traps in genome-wide data sets: case examples from yeast. Nat. Rev. Genet. **3**:653–661.
26. **Hughes TR, Roberts CJ, Dai H, Jones AR, Meyer MR, Slade D, Burchard J, Dow S, Ward TR, Kidd MJ, Friend SH, Marton MJ.** 2000. Widespread aneuploidy revealed by DNA microarray expression profiling. Nat. Genet. **25**:333–337.
27. **Barbour L, Ball LG, Zhang K, Xiao W.** 2006. DNA damage checkpoints are involved in postreplication repair. Genetics **174**:1789–1800.
28. **Daigaku Y, Davies AA, Ulrich HD.** 2010. Ubiquitin-dependent DNA damage bypass is separable from genome replication. Nature **465**:951–955.
29. **Barbour L, Xiao W.** 2003. Regulation of alternative replication bypass pathways at stalled replication forks and its effects on genome stability: a yeast model. Mutat. Res. **532**:137–155.
30. **Gangavarapu V, Prakash S, Prakash L.** 2007. Requirement of RAD52 group genes for postreplication repair of UV-damaged DNA in Saccharomyces cerevisiae. Mol. Cell. Biol. **27**:7758–7764.
31. **Paulovich AG, Hartwell LH.** 1995. A checkpoint regulates the rate of progression through S phase in *S. cerevisiae* in response to DNA damage. Cell **82**:841–847.
32. **Lopes M, Foiani M, Sogo JM.** 2006. Multiple mechanisms control chromosome integrity after replication fork uncoupling and restart at irreparable UV lesions. Mol. Cell **21**:15–27.
33. **Prakash L.** 1981. Characterization of postreplication repair in Saccharomyces cerevisiae and effects of rad6, rad18, rev3 and rad52 mutations. Mol. Gen. Genet. **184**:471–478.
34. **Geigl EM, Eckardt-Schupp F.** 1991. The repair of double-strand breaks and S1 nuclease-sensitive sites can be monitored chromosome-specifically in Saccharomyces cerevisiae using pulse-field gel electrophoresis. Mol. Microbiol. **5**:1615–1620.
35. **Ma W, Panduri V, Sterling JF, Van Houten B, Gordenin DA, Resnick MA.** 2009. The transition of closely opposed lesions to double-strand breaks during long-patch base excision repair is prevented by the coordinated action of DNA polymerase δ and Rad27/Fen1. Mol. Cell. Biol. **29**:1212–1221.
36. **Chu G, Vollrath D, Davis RW.** 1986. Separation of large DNA molecules by contour-clamped homogeneous electric fields. Science **234**:1582–1585.
37. **Karras GI, Jentsch S.** 2010. The *RAD6* DNA damage tolerance pathway operates uncoupled from the replication fork and is functional beyond S phase. Cell **141**:255–267.
38. **Giannattasio M, Follonier C, Tourrière H, Puddu F, Lazzaro F, Pasero P, Lopes M, Plevani P, Muzi-Falconi M.** 2010. Exo1 competes with repair synthesis, converts NER intermediates to long ssDNA gaps, and promotes checkpoint activation. Mol. Cell **40**:50–62.
39. **Pfander B, Moldovan GL, Sacher M, Hoege C, Jentsch S.** 2005. SUMO-modified PCNA recruits Srs2 to prevent recombination during S phase. Nature **436**:428–433.
40. **Hishida T, Hirade Y, Haruta N, Kubota Y, Iwasaki H.** 2010. Srs2 plays a critical role in reversible G_2 arrest upon chronic and low doses of UV irradiation via two distinct homologous recombination-dependent mechanisms in postreplication repair-deficient cells. Mol. Cell. Biol. **30**:4840–4850.
41. **Liu J, Renault L, Veaute X, Fabre F, Stahlberg H, Heyer WD.** 2011. Rad51 paralogues Rad55-Rad57 balance the antirecombinase Srs2 in Rad51 filament formation. Nature **479**:245–248.
42. **Zhang H, Lawrence CW.** 2005. The error-free component of the *RAD6/RAD18* DNA damage tolerance pathway of budding yeast employs sister-strand recombination. Proc. Natl. Acad. Sci. U. S. A. **102**:15954–15959.
43. **Waters LS, Walker GC.** 2006. The critical mutagenic translesion DNA polymerase Rev1 is highly expressed during G(2)/M phase rather than S phase. Proc. Natl. Acad. Sci. U. S. A. **103**:8971–8976.
44. **Broomfield S, Hryciw T, Xiao W.** 2001. DNA postreplication repair and mutagenesis in *Saccharomyces cerevisiae*. Mutat. Res. **486**:167–184.
45. **Toczyski DP, Galgoczy DJ, Hartwell LH.** 1997. *CDC5* and CKII control adaptation to the yeast DNA damage checkpoint. Cell **90**:1097–1106.
46. **Segurado M, Diffley JF.** 2008. Separate roles for the DNA damage checkpoint protein kinases in stabilizing DNA replication forks. Genes Dev. **22**:1816–1827.
47. **Claus EB, Calvocoressi L, Bondy ML, Schildkraut JM, Wiemels JL, Wrensch M.** 2012. Dental X-rays and risk of meningioma. Cancer **118**:4530–4537.
48. **Longstreth WT, Jr, Phillips LE, Drangsholt M, Koepsell TD, Custer BS, Gehrels JA, van Belle G.** 2004. Dental X-rays and the risk of intracranial meningioma: a population-based case-control study. Cancer **100**:1026–1034.
49. **Nguyen PK, Wu JC.** 2011. Radiation exposure from imaging tests: is there an increased cancer risk? Expert Rev. Cardiovasc. Ther. **9**:177–183.
50. **Brenner DJ.** 2009. Extrapolating radiation-induced cancer risks from low doses to very low doses. Health Phys. **97**:505–509.
51. **Goodhead DT.** 2010. New radiobiological, radiation risk and radiation protection paradigms. Mutat. Res. **687**:13–16.
52. **Mullenders L, Atkinson M, Paretzke H, Sabatier L, Bouffler S.** 2009. Assessing cancer risks of low-dose radiation. Nat. Rev. Cancer **9**:596–604.
53. **Preston DL, Pierce DA, Shimizu Y, Cullings HM, Fujita S, Funamoto S, Kodama K.** 2004. Effect of recent changes in atomic bomb survivor dosimetry on cancer mortality risk estimates. Radiat. Res. **162**:377–389.
54. **Preston DL, Ron E, Tokuoka S, Funamoto S, Nishi N, Soda M, Mabuchi K, Kodama K.** 2007. Solid cancer incidence in atomic bomb survivors: 1958–1998. Radiat. Res. **168**:1–64.
55. **Baerlocher MO, Detsky AS.** 2010. Discussing radiation risks associated with CT scans with patients. JAMA **304**:2170–2171.
56. **Brenner DJ, Hall EJ.** 2007. Computed tomography—an increasing source of radiation exposure. N. Engl. J. Med. **357**:2277–2284.